

Effects of Temperature and Gas Atmosphere during Coal Tar Pitch Emulsification on The Characteristics of Mesocarbon Microbeads (MCMB) as Battery Anode Precursor

Nurulhuda Halim^{1,*}, Fabian Renaldi¹, Ismi Handayani¹, and Edy Sanwani¹

¹Department of Metallurgical Engineering, Faculty of Mining and Petroleum Engineering, Institut Teknologi Bandung, Bandung 4132, Indonesia

Abstract. Mesocarbon microbeads (MCMB) are spherical carbon materials characterized by their high crystallinity and excellent electrochemical properties, making them attractive for energy storage applications. This study investigates the effects of temperature and gas atmosphere during coal tar pitch (CTP) emulsification on the characteristics of MCMB as precursors for battery anodes. Coal tar (CT) was distilled under vacuum and atmospheric conditions to produce CTP-V and CTP-A, respectively. The pitches were characterized for ash, quinoline insolubles (QI), toluene insolubles (TI), softening point, and ultimate composition. Emulsification was performed by mixing CTP with silicone oil, heating at 290 °C or 360 °C under air, N₂, or CO₂ flow, followed by mesophase (MP) separation and carbonization at 900 °C to obtain MCMB. Results showed that CTP-V, with a higher softening point (151 °C) and QI (5.02%), was more suitable for MCMB synthesis than CTP-A, although its high TI content contributed to irregular morphologies. Increasing the emulsification temperature in N₂ and CO₂ atmospheres improved carbon crystallinity and produced larger MCMB particles, while air at 360 °C prevented MCMB formation due to crosslinking reactions. The most promising sample (M-290A) exhibited improved crystallinity (L_c = 2.178 nm, N = 7.148).

1 Introduction

The demand for energy storage technologies, such as lithium batteries (LiBs), has grown rapidly over the past decade. Global battery demand is projected to reach approximately 5.5 TWh by 2030 and exceed 9 TWh by 2040, in line with the accelerated transition to clean energy [1]. One of the most critical components of LiBs is the anode, which is commonly fabricated from graphite due to its small surface change, structural stability during cycling, high energy density, and relatively low cost [2]. In terms of quality and performance consistency, synthetic graphite is superior to natural graphite, and its production from industrial byproducts can reduce waste while providing a high-performance feedstock [2].

One of the most common and suitable types of synthetic graphite for use as a battery anode precursor is mesocarbon microbead (MCMB). MCMBs are selected as anode precursors because of their uniform spherical morphology and a structure that can be readily modified to enhance their lithium-ion storage and transport capabilities. MCMB can be produced via mesothermal liquid-phase pyrolysis of polycyclic aromatic hydrocarbons (PAH), such as coal tar pitch (CTP), at temperatures above 400 °C to form a mesophase (MP), which is subsequently separated from the pitch through solvent extraction [3]. CTP contains a large amount of PAH, enabling the production of solid carbon with high

yield as well as morphology and structural ordering suitable for MCMB precursors.

The emulsification method is one of the effective approaches for MCMB synthesis, producing products with uniform and stable spherical morphology [4]. In the study by Kodama et al. (1992) [4], the use of CTP with a high softening point at 307 °C produced a stable morphology; however, the process required an additional 5 hours of oxidation for stabilization before carbonization, making it less efficient in terms of cost and production time. Furthermore, Yuan et al. (2020) [5] utilized CTP with a low softening point at 85 °C to produce pitch carbon beads (PCB) through emulsification combined with gas blowing (compressed air or nitrogen), to achieve simultaneous spheroidization and stabilization. The experiment produced a spherical morphology under an air atmosphere, as oxidation facilitated the formation of crosslinking structures, but not under a nitrogen atmosphere, which does not promote crosslinking. The limited number of comprehensive studies on the interplay between gas atmosphere and temperature variation in crosslinking formation remains a major challenge, highlighting the need for further investigation to optimize this process.

This study aims to examine the effects of gas atmosphere variation (carbon dioxide, nitrogen, and air) and temperature on the emulsification and stabilization processes of MCMB. In addition, it explores the role of the gas atmosphere in crosslinking formation, which

* Corresponding author: nurulhuda.halim@itb.ac.id

contributes to the stabilization of spherical morphology and the enhancement of MCMB crystallinity. By elucidating the interplay among gas atmosphere, temperature, crosslinking formation, and crystallinity, this work seeks to identify optimal conditions that improve both process efficiency and the quality of MCMB as an anode material for lithium-ion batteries.

2 Materials and methods

2.1 Materials and sample preparation

Coal tar (CT) was obtained from a coking plant in Cilegon, Banten Province, Indonesia. The CT was distilled under either vacuum or atmospheric conditions to produce coal tar pitch (CTP), denoted as CTP-V and CTP-A, respectively. Vacuum distillation was performed by gradually heating the CT to 360 °C under reduced pressure (~0.1 atm), while atmospheric distillation was carried out at ambient pressure using similar heating stages. The resulting CTP-V and CTP-A samples were characterized for ash content, quinoline insoluble (QI), toluene insoluble (TI), softening point, and ultimate composition.

During emulsification, CTP-V or CTP-A was mixed with silicone oil at a mass ratio of 1:50 (CTP:silicone oil). The mixture was heated to either 290 °C or 360 °C at a rate of 2 °C/min while stirring at 800 rpm. A continuous gas flow of air, nitrogen, or carbon dioxide (500 mL/min) was introduced for 3 h to promote mesophase (MP) formation. Figure 1 presents the schematic of the emulsification process. The MP was separated from the silicone oil by centrifugation and dried in a vacuum oven at 70 °C for 19 h. The dried MP was then carbonized at 900 °C for 2 h in a nitrogen atmosphere using a tube furnace to produce mesocarbon microbeads (MCMB). The resulting samples were denoted as MP-XY for mesophase, and M-XY for MCMB, where X represents the emulsification temperature (°C) and Y denotes the gas atmosphere (N = N₂, A = air, C = CO₂).

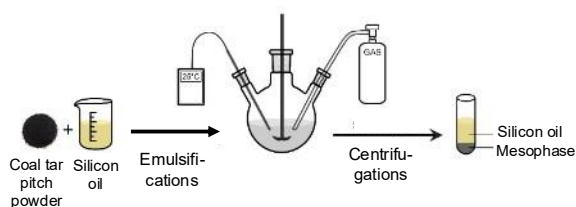


Fig. 1. Emulsification procedure of coal tar pitch

2.2 Sample characterization

The CT, CTP-V, and CTP-A samples were further characterized to determine thermal properties and composition. Standard methods were applied, including ASTM D2415-98 for ash content, ASTM D2318-98 for QI, ASTM D36/36M-14 for softening point, and ASTM D4312-95a for TI. Ultimate analysis of CTP-V followed ASTM D3176-15.

The MCMB samples were characterized using multiple techniques. Morphological analysis was

conducted using scanning electron microscopy (SEM; Thermo Fisher Scientific, Apreo 2 C HiVac) to examine particle shape and size distribution. Fourier transform infrared spectroscopy (FTIR; Shimadzu IR Prestige-21) was performed in the range of 4500 – 400 cm⁻¹ with 4 cm⁻¹ resolution and 40 scans to identify functional groups.

2.3 XRD characterization

X-ray diffraction (XRD) analysis (Rigaku MiniFlex 600-C, Cu K α radiation, $\lambda = 0.154$ nm) was used to assess the crystallinity of MCMB. The interlayer spacing (d_{002}), stacking height (L_c), and average number of layers (N) were calculated using the following equations:

$$d_{002} = \frac{\lambda}{2 \times \sin\theta_{002}} \quad (1)$$

$$L_c = \frac{0.9 \times \lambda}{\beta_{002} \times \cos\theta_{002}} \quad (2)$$

$$N = \frac{L_c}{d_{002}} + 1 \quad (3)$$

where λ is the X-ray wavelength (0.154 nm), β_{002} is the full width at half maximum (FWHM) of the 002 reflection, and θ_{002} is the diffraction angle.

3 Results and discussion

3.1 Coal tar and coal tar pitch properties

Proximate analysis was conducted for CT, CTP-A, and CTP-V. As shown in Table 1, the softening points of CTP-A and CTP-V were 59.5 °C and 151 °C, respectively. CTP-V was selected for emulsification because its softening point falls within the ideal range of 110 – 150 °C [6]. The ash contents of CT and CTP were below 1%, with CT and CTP-V showing values of 0.04% and 0.2%, both within the acceptable range (<0.5%). The QI values of CT, CTP-V, and CTP-A were 2.2%, 5.02%, and 2.77%, respectively. The QI content of CTP-V lies within the recommended range [7]. TI values for CT, CTP-V, and CTP-A were 7.8%, 65.76%, and 29.09%, respectively. The high TI content of CTP-A suggests a tendency to promote bulk mesophase formation during emulsification and carbonization.

The ultimate analysis of CTP-V (Table 2) shows a C/H ratio of 1.52, indicating a relatively high aliphatic content and suboptimal aromaticity for forming stable MCMB.

Table 1. Tar and tar pitch properties.

Sample	Ash, adb (%)	QI (%)	TI (%)	Softening Point (°C)	Yield (%)
CT	0.04	2.20	7.80	-	-
CTP-V	0.20	5.02	65.76	151	26
CTP-A	0.08	2.77	29.09	59.5	43.8

Table 2. Ultimate analysis of tar pitch in a vacuum distillation.

Sample	C (%)	H (%)	N (%)	S (%)	O (%)	C/H
CTP-V	85.32	4.70	1.29	0.55	7.86	1.52

3.2 Effect of distillation conditions on CTP properties

The influence of distillation conditions on CTP characteristics is summarized in Table 1. The CTP-V yield was 26%, while CTP-A yielded 43.8%. This difference is attributed to the greater removal of light and middle fractions during vacuum distillation, leaving less pitch residue. Yield variation was accompanied by differences in TI, QI, and softening point values. TI increased to 65.76% in CTP-V and 29.09% in CTP-A, compared with 7.8% in CT. Similarly, QI rose to 5.02% in CTP-V and 2.77% in CTP-A, compared with 2.2% in CT. These increases probably result from the formation of secondary insolubles during heating above 350 °C, when aromatic components polymerize and condense into more complex structures [8].

Softening points also differed: 151 °C for CTP-V versus 59.5 °C for CTP-A. Vacuum distillation removes volatile fractions at lower temperatures than conventional distillation, reducing low-molecular-weight components that lower the softening point. Consequently, the average molecular weight and insoluble fractions (QI and TI) increase. Vacuum conditions also minimize hydrocarbon cracking, which is more prevalent in conventional distillation, and promote mesophase particle formation. Thus, the higher softening point, QI, and TI of CTP-V are attributed to vacuum processing.

3.3 Effect of emulsification temperature on MCMB properties

Emulsification temperature significantly affects the morphology, crystallinity, and functional groups of MCMB. The chosen temperatures, 290 °C and 360 °C, were based on the TGA of CTP-V in air (Figure 3). A mass increase between 30-216 °C reflected oxygen group formation, while mass loss between 216 – 420 °C indicated decomposition of light components. Beyond 420 °C, the mass stabilized, signifying the completion of crosslinking. Thus, 290 °C and 360 °C were selected as representative crosslinking conditions.

At 360 °C in air, additional crosslinking occurred between Si-O bonds in silicone oil and oxygen, leading to gelation. The commercial silicone oil used in this study lacked thermal stability compared to phenyl-based silicone oils (>350 °C), which are more commonly recommended. Gelation reduced fluidity and prevented mesophase formation, producing a gel-like material (Figure 2d).

SEM results (Figure 5) showed that increasing the emulsification temperature enlarged MCMB particle size under both CO₂ (from 2.51 to 7.11 μm) and N₂ (from 2.21 to 6.25 μm) atmospheres. Higher temperatures accelerate sphere growth and coalescence, yielding larger particles [9]. XRD patterns (Figure 4a)

displayed a main diffraction peak near 26°, corresponding to graphite (002) [9]. Data in Table 3 also show that increasing temperature under N₂ and CO₂ enhanced crystallinity, as reflected in higher *L_c* and *N* values. This is explained by increased molecular mobility, which improves the orientation and aromatization of pitch molecules, leading to more ordered carbon structures [9].

FTIR spectra (Figure 4b) revealed common functional groups: O–H (3200 – 3600 cm⁻¹), aliphatic C–H (2850 – 2970 cm⁻¹), aromatic C=C (1600 – 1700 cm⁻¹), and aromatic C–H (900 – 750 cm⁻¹). The limited oxygen groups suggest effective decomposition of carbonyl and carboxyl groups during carbonization, producing stable carbon.

Table 3. XRD parameter of all samples.

Sample	<i>d</i> ₀₀₂ (nm)	<i>L_c</i> (nm)	<i>N</i>	FWHM 002 (°)
M-290A	0.354	2.178	7.148	3.734
M-360A	-	-	-	-
M-290C	0.345	1.011	3.932	8.057
M-360C	0.354	1.219	4.442	6.671
M-290N	0.373	1.071	3.874	7.574
M-360N	0.361	1.410	4.906	5.764

3.4 Effect of gas atmosphere emulsification on MCMB properties

The gas atmosphere also influenced MCMB properties. SEM analysis showed average particle sizes of 2.72 μm (M-290A), 2.42 μm (M-290C), and 2.22 μm (M-290N). Larger particles benefit LiB anodes by enhancing capacity and cycle life, whereas smaller particles increase conductivity but also defects [10]. MCMB formed under N₂ and CO₂ showed irregular lamellar structures with micropores (Figure 5), likely caused by gas release from decomposition of alkyl side chains and light components.

XRD results (Table 3) indicate that M-290A had the highest crystallinity, with the smallest FWHM and highest *L_c* and *N*. This suggests that oxidation during emulsification stabilized the lamellar structure, which was retained during carbonization. However, M-290A also showed a larger interlayer spacing (*d*₀₀₂), due to decomposition of oxygen groups, which induced internal strain [3]. In the context of its application as an anode precursor, the interlayer spacing of carbon has a significant influence on both the electrical conductivity and lithium-ion storage capacity in LiBs. A smaller *d*₀₀₂ value, around 0.3354 nm, provides high electrical conductivity and structural stability comparable to natural graphite, whereas larger *d*₀₀₂ value (0.34 – 0.37 nm) enhances lithium storage capacity but leads to a more rapid decline in charge–discharge capacity during cycling, caused by disordered and non-crystalline MCMB domains, random lattice structures, and metallic impurity contamination that can induce compositional changes during cycling [11].

FTIR spectra confirmed similar groups across all atmospheres (O–H, aliphatic C–H, aromatic C=C, C–O,

and aromatic C–H). Although air promotes oxygenated groups, these decompose during carbonization [12]. In contrast, N₂ is inert, and CO₂ oxidation is limited at 290 °C because of its high stability, rendering it less reactive at relatively low temperatures. Overall, TGA, SEM, and XRD analyses identify 290 °C in air as the optimal condition for producing MCMB with the most ordered crystalline structure and defect-free morphology.

3.5 Evaluation of the characteristics of MCMB under optimal conditions

The morphology of the MCMB obtained in this study, as shown in Figure 5, indicates that the spheres did not develop into perfectly spherical shapes. This is likely attributable to the high TI content at 65% of the CTP-V used for emulsification. Secondary TI formed during high-temperature distillation (>350 °C) attaches side groups to aromatic rings, hindering alignment and producing disordered spheres [13].

TI dynamics are closely linked to treatment conditions. At lower temperatures, TI decreases as large molecules decompose; above 360 °C, TI increases again via secondary polymerization and aggregation of oxygen-rich compounds. This trend is consistent with Du et al. (2017), who observed similar behavior in hydrocracking of coal tar at hydrogen pressures of 8 – 12 MPa and temperatures of 320 – 440 °C. At lower temperatures, large TI molecules decompose into smaller, toluene-soluble species [13]. However, when the temperature exceeds 360 °C, TI content rises again due to the formation of secondary TI through the polymerization and aggregation of oxygen-rich compounds such as asphaltenes. These findings highlight TI's critical role in structural development during thermal processing.

Moreover, the morphological characteristics of carbon obtained through the emulsification process were found to be significantly influenced by parameters such as temperature, duration, and the presence of surfactants. These results can be compared with the study of Yuan et al. (2020), who synthesized PCB using an emulsification technique combined with gas blowing (nitrogen and air) at 220 – 280 °C. In that study, low-softening-point pitch at 85 °C with a TI content of 49.84% was employed together with the surfactant sodium dodecyl benzene sulfonate (SDBS), which was shown to effectively reduce interfacial tension and produce stable, spherical pitch droplets [5]. In contrast, in the present study, the absence of surfactants such as SDBS resulted in MCMB that tended to coalesce and failed to develop into perfect spherical structures. This finding indicates that emulsion stability remains strongly governed by the interfacial conditions established during the emulsification process.

Further analysis of the treatment temperature revealed differences in the optimal temperature for the formation of spherical carbon morphologies. The optimal morphology in this study was obtained at 290 °C (M-290A), corresponding to early crosslinking. This differs from Yuan et al. (2020), who reported an optimal 260 °C, highlighting that the “best” temperature depends on achieving sufficient crosslinking rather than reaching

the highest thermal point [5]. This discrepancy suggests that the optimal temperature is not solely determined by reaching the highest temperature, but rather by its ability to establish thermal conditions sufficient to initiate crosslinking network formation prior to carbonization. Consequently, both the dynamics of TI development and the final morphology of MCMB are governed by the complex interplay among temperature, residence time, the presence of emulsifying agents, and the intrinsic structural characteristics of the initial pitch. Crystallinity of M-290A remained suboptimal ($d_{002} = 0.354$ nm; $L_c = 2.178$ nm; $N = 7.148$).

3.6 Result comparison

Compared with Cheng et al. (2009) [12] and Fang et al. (2015) [11], who reported much higher L_c values after graphitization at 2300 – 3000 °C, by conducting graphitization of MCMB to produce spherical mesophase graphite, and mesophase synthesized using an emulsion method with phenyl silicone oil at 350 °C for two hours under a nitrogen flow, followed by graphitization of the resulting mesophase, respectively. M-290A consisted of thinner, less ordered carbon layers. This likely reduces conductivity due to restricted electron mobility.

As shown in Table 4, natural and synthetic graphite (Badenhorst et al., 2020) [14] and commercial graphite (Cabielles et al., 2009) [15], exhibit far superior crystallinity. Their performance was achieved through high-temperature graphitization (2300 – 3000 °C), consistent with Cheng et al. (2009) and Fang et al. (2015). Therefore, further graphitization at elevated temperatures is required to enhance MCMB crystallinity and make it suitable as a lithium-ion battery anode precursor.

Table 4. Comparison of d_{002} , L_c , and N parameters of MCMB M290-A with various previous studies.

References	Starting material	d_{002} (nm)	L_c (nm)	N
This study	Coal tar pitch (heating at 290 °C)	0.354	2.178	7.148
Cheng, et al. [12]	coal tar pitch (heating at 420 °C)	0.336	25.35	-
Fang, et al. [11]	mesophase graphite (heating at 3000 °C)	0.337	20.7	-
Badenhorst, et al. [14]	Natural graphite	0.335	33.9	101
	Graphitized demineralised char concentrate	0.336	44.6	133
Cabielles, et al. [15]	Commercial synthetic graphites	0.336	25.8	-

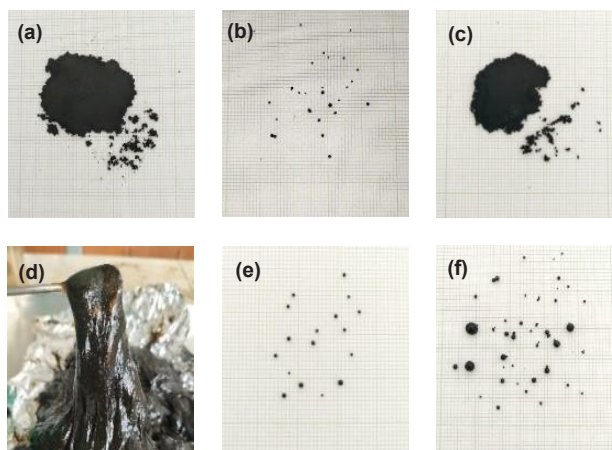


Fig. 2. (a) MP-290A, (b) MP-290C, (c) MP-290N, (d) MP-360A, (e) MP-360C, and (f) MP-360N.

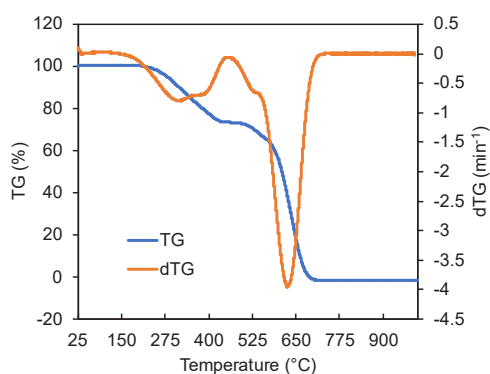


Fig. 3. TG-DSC graph of CTP-V.

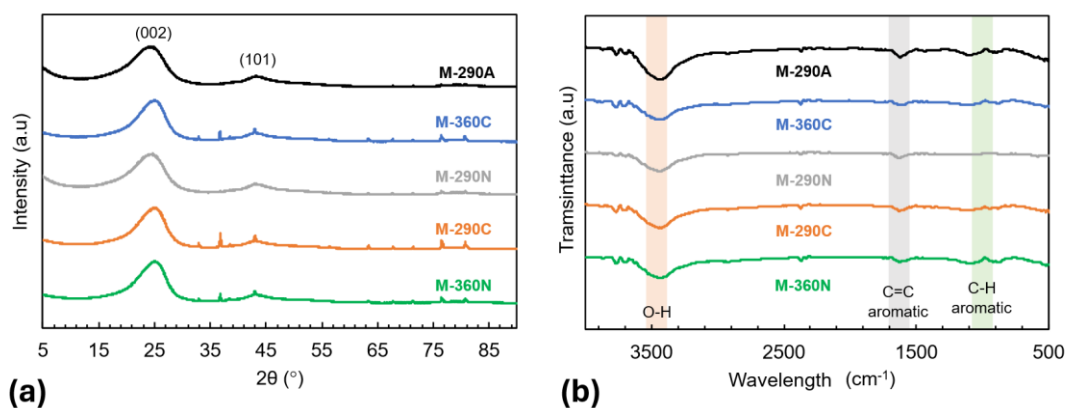


Fig. 4. (a) XRD spectrum of MCMB, and (b) FTIR spectrum of MCMB

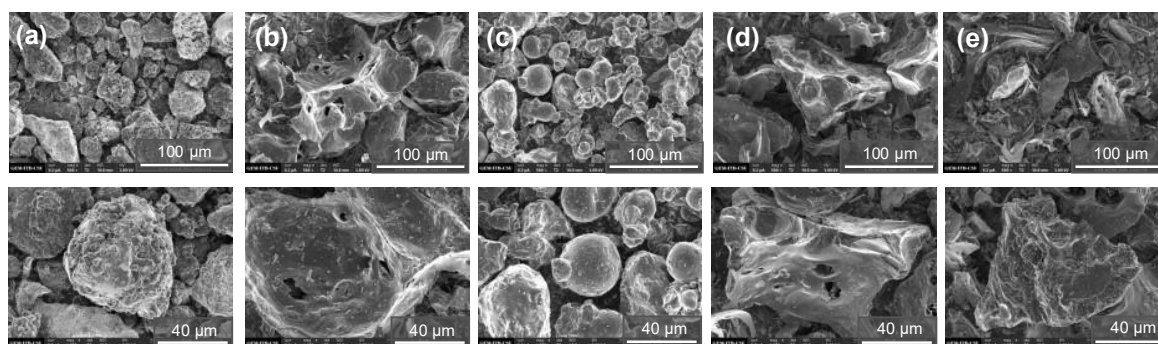


Fig. 5. SEM images of (a) M-290A, (b) M-290C, (c) M-290N, (d) M-360C, and (e) M-360N at 500 times (top) and 1000 times (bottom) magnifications.

4 Conclusion

1. Vacuum distillation produced CTP-V with a softening point of 151 °C, QI content of 5.02%, and TI content of 65%. In contrast, conventional distillation yielded CTP-A with a softening point of 59.5 °C, QI content of 2.8%, and TI content of 28%. Based on softening point and QI, CTP-V is more suitable as an MCMB precursor. However, its high TI content likely contributed to the imperfectly spherical morphology of the resulting MCMB.
2. Under nitrogen and carbon dioxide atmospheres, raising the emulsification temperature from 290 °C to 360 °C increased MCMB particle size and improved carbon crystallinity, as indicated by higher Lc and N values. In contrast, emulsification in air at 360 °C produced a gel-like material due to crosslinking between Si–O bonds in silicone oil and oxygen, preventing MCMB formation. Temperature variation did not markedly affect the functional groups of the five MCMB samples, indicating limited impact on their chemical structure.
3. At 290 °C, emulsification in air yielded larger MCMB particles and a more ordered crystal structure than those synthesized in nitrogen and carbon dioxide, or even at 360 °C. The best sample (M-290A) exhibited Lc = 2.178 nm and N = 7.148. Differences in gas atmosphere had little effect on functional groups, and although air promoted oxygenated groups, these were likely decomposed during carbonization at 900 °C.
4. Despite showing the most favorable parameters, M-290A did not meet the requirements for an anode precursor. Its morphology was irregular, and its crystal structure remained below specification, with d002 = 0.354 nm (above the commercial graphite range of 0.3359 – 0.3367 nm) and Lc = 2.178 nm (well below the 25.35 – 62.7 nm range).

References

1. IEA: Batteries and Secure Energy Transitions. IEA, Paris (2024) <https://www.iea.org/reports/batteries-and-secure-energy-transitions>
2. H. Zhang, Y. Yang, D. Ren, L. Wang, and X. He: Graphite as anode materials: Fundamental mechanism, recent progress and advances. *Energy Storage Mater.* **36**, 147 – 170 (2021). <https://doi.org/10.1016/j.ensm.2020.12.027>
3. L. Li, X. lin, J. He, Y. Zhang, J. Lv, and Y. Wang: Preparation of mesocarbon microbeads from coal tar pitch with blending of biomass tar pitch. *J. Anal. Appl. Pyrolysis.* **155**, 105039 (2021). <https://doi.org/10.1016/j.jaap.2021.105039>
4. M. Kodama, T. Fujiura, K. Esumi, K. Meguro, and H. Honda: Carbonization and graphitization of meso-carbon microbeads prepared by the emulsion method. *J. Mater. Sci.* **27**, 6079 – 6085 (1992). <https://doi.org/10.1007/BF01133753>
5. M. Yuan, B. Cao, C. Meng, H. Zuo, A. Li, Z. Ma, X. Chen, and H. Song: Preparation of pitch-based carbon microbeads by a simultaneous spheroidization and stabilization process for lithium-ion batteries. *Chem. Eng. J.* **400**, 125948 (2020). <https://doi.org/10.1016/j.cej.2020.125948>
6. W. Boenigk, C. Kuhnt, J. Stiegert, J. Claes, and L. Edwards: Pilot Anode Properties of Binder Pitches Softening Between 110 and 150 °C. In: *Light Metals 2017*. pp. 1357 – 1364. Springer (2017) https://doi.org/10.1007/978-3-319-51541-0_139
7. D. Kocaefe, J. Bureau, Y. Kocaefe, and A. Rastegari: Impact of Pitch Modification on Anode Properties: Effect of Additive Type. *ACS Omega.* **8**, 25467 – 25477 (2023). <https://doi.org/10.1021/acsomega.3c02978>
8. M.S. Hosseini, and P. Chartrand: Modeling the Coal Tar Pitch Primary Carbonization Process. *Fuels.* **3**, 698 – 729 (2022). <https://doi.org/10.3390/fuels3040042>
9. X. Zhang, Z. Ma, Y. Meng, M. Xiao, B. Fan, H. Song, and Y. Yin: Effects of the addition of conductive graphene on the preparation of mesophase from refined coal tar pitch. *J. Anal. Appl. Pyrolysis.* **140**, 274 – 280 (2019). <https://doi.org/10.1016/j.jaap.2019.04.004>
10. D. Coetzee, M. Venkataraman, J. Militky, and M. Petru: Influence of nanoparticles on thermal and electrical conductivity of composites. *Polymers (Basel).* **12**, (2020). <https://doi.org/10.3390/POLYM12040742>
11. M.D. Fang, T.H. Ho, J.P. Yen, Y.R. Lin, J.L. Hong, S.H. Wu, and J.J. Jow: Preparation of advanced carbon anode materials from mesocarbon microbeads for use in high C-rate lithium ion batteries. *Materials (Basel).* **8**, 3550 – 3561 (2015). <https://doi.org/10.3390/ma8063550>
12. Y.L. Cheng, T.H. Li, H. Li, and D.Q. Jing: Preparation of mesocarbon microbeads and microstructure evolution. *Proc. Int. Symp. Phys. Fail. Anal. Integr. Circuits, IPFA.* 559 – 562 (2009). <https://doi.org/10.1109/IPFA.2009.5232583>
13. J. Du, W. Deng, J. Li, C. Li, F. Du, Z. Zhang, T. Yang, Q. Sun, and X. Cao: Structural and compositional evolution of coal tar toluene insoluble during slurry-phase hydrocracking. *Fuel.* **203**, 352 – 359 (2017). <https://doi.org/10.1016/j.fuel.2017.04.139>
14. C. Badenhorst, C. Santos, J. Lázaro-Martínez, B. Bialecka, M. Cruceu, A. Guedes, R. Guimarães, K. Moreira, G. Predeanu, I. Suárez-Ruiz, I. Cameán, B. Valentim, and N. Wagner: Assessment of graphitized coal ash char concentrates as a potential synthetic graphite source. *Minerals.* **10**, (2020). <https://doi.org/10.3390/min10110986>
15. M. Cabielles, J.N. Rouzaud, and A.B. Garcia: High-Resolution Transmission Electron Microscopy Studies of Graphite Materials Prepared by High-Temperature Treatment of Unburned Carbon Concentrates from Combustion Fly Ashes. *Energy and Fuels.* **23**, 942 – 950 (2009). <https://doi.org/10.1021/ef800763s>